Proc. Natl. Acad. Sci. USA
Vol. 95, pp. 9524–9529, August 1998
Medical Sciences

A mouse model of severe von Willebrand disease: Defects in hemostasis and thrombosis

CÉCILE DENIS*†, NASSIA METHIA*†, PAUL S. FRENETTE*‡, HELEN RAYBURN¶, MOLLIE ULLMAN-CULLERÉ¶, RICHARD O. HYNES§¶, AND DENISA D. WAGNER*†‖

*The Center for Blood Research and Departments of †Pathology and ‡Medicine, Harvard Medical School, Boston, MA 02115; and §Howard Hughes Medical Institute and ¶Center for Cancer Research, Department of Biology, Massachusetts Institute of Technology, Cambridge, MA 02139

Contributed by Richard O. Hynes, June 2, 1998

ABSTRACT **von Willebrand factor (vWf) deficiency causes severe von Willebrand disease in humans. We generated a mouse model for this disease by using gene targeting. vWf-deficient mice appeared normal at birth; they were viable and fertile. Neither vWf nor vWf propolypeptide (von Willebrand antigen II) were detectable in plasma, platelets, or endothelial cells of the homozygous mutant mice. The mutant mice exhibited defects in hemostasis with a highly prolonged bleeding time and spontaneous bleeding events in ≈10% of neonates. As in the human disease, the factor VIII level in these mice was reduced strongly as a result of the lack of protection provided by vWf. Defective thrombosis in mutant mice was also evident in an *in vivo* model of vascular injury. In this model, the exteriorized mesentery was superfused with ferric chloride and the accumulation of fluorescently labeled platelets was observed by intravital microscopy. We conclude that these mice very closely mimic severe human von Willebrand disease and will be very useful for investigating the role of vWf in normal physiology and in disease models.**

von Willebrand disease (vWd) is the most common inherited bleeding disorder. A large number of vWd subtypes have been defined, but all forms of the disease involve quantitative or qualitative defects in pro-von Willebrand factor (vWf) (1). vWf is required for the normal adhesion of platelets to the subendothelium, a crucial step in primary hemostasis (2). vWf also plays a role in coagulation by stabilizing factor VIII (FVIII) and by protecting it against proteolytic inactivation (3). The role of the large vWf propolypeptide, von Willebrand antigen II, found in plasma, is not known. Type 3 vWd, also known as severe vWd, is characterized by an absence of vWf in all of the different compartments where vWf is normally found: plasma, platelets, endothelial cells, and subendothelium. Type 3 vWd is rare, with an incidence of one per million individuals, and produces major defects in both primary hemostasis and coagulation. Animal models of type 3 vWd have been described in the dog and pig (4). Studies in the pig have been very useful to characterize vWf function, but, apart from the obvious problems related to the size and cost of the animals, this model was not ideal because homozygous pigs are not totally deficient in vWf (5). Furthermore, the pig colony is not syngeneic, making it difficult to study the importance of vWf in diseases involving many gene products such as atherosclerosis, in which its role is still controversial (6).

vWf is known to be involved in thrombus formation, as demonstrated by studies made in flow using perfusion chambers and aggregometer (7, 8). Therefore, vWf is likely to play a role in diseases in which either platelet adhesion or thrombus formation plays a role, such as disseminated intravascular coagulation, thrombotic thrombocytopenic purpura, stroke, cancer metastasis, sickle cell disease, and glomerular nephritis. The precise role played by vWf in the above diseases remains to be established, and a small animal model of vWd would be very helpful. To generate such a model, we have disrupted the vWf gene in mice. We report that the mutant mice are fully deficient in pro-vWf and that they represent a very close model of the human type 3 vWd. In addition, to define the role of vWf in thrombus formation, we developed an *in vivo* thrombosis model, allowing us to observe platelet deposition in injured vessels by intravital microscopy.

METHODS

Construction of the Targeting Vector and Generation of vWf-Deficient Mice. A 161-bp probe overlapping exons 4 and 5 of human vWf cDNA, which encode part of the D1 domain of the vWf propolypeptide, was used to screen a 129/Sv genomic library (Stratagene). Three genomic clones were isolated, and a 7.3-kb *Bam*HI fragment from one of these clones was identified as containing exons 4 and 5 of vWf by Southern blot and sequencing. The targeting vector was constructed by removing an 800-bp *Kpn*I–*Cla*I fragment including exons 4 and 5 and replacing it with a 1.7-kb phosphoglycerate kinase neomycin (neo) cassette in the opposite transcriptional orientation to the vWf gene. Flanking the neo cassette, a 2.1-kb sequence (*Sma*I–*Kpn*I) and a 3.8-kb fragment (*Cla*I–*Sma*I) were included upstream and downstream, respectively. The resulting 7.6-kb fragment was inserted between two herpes simplex virus thymidine kinase cassettes (Fig. 1*A*). The final 15.9-kb construct was linearized with *Not*I and introduced into D3 embryonic stem (ES) cells by electroporation, and stable transfectants were selected as described (9). Individual ES clones were screened for homologous recombination by Southern blot analysis by using as a probe a 600-bp *Bam*HI-*Sma*I genomic fragment upstream of the targeting construct (Fig. 1*A*). Targeted ES cells were microinjected into the blastocoele cavity of C57BL/6J blastocysts and were implanted into pseudopregnant females (10). Chimeric males thus generated were bred to C57BL/6J females to produce heterozygous vWf +/− offspring. Genotypes of mice were obtained by Southern blot by using tail biopsy DNA, as described above.

Northern Blot Analysis. Total RNA from heart and lung was isolated by using RNA-Stat 60 (Tel-Test, Friendswood, TX). Between 15 and 20 μg of total RNA was electrophoresed on a 1.2% agarose gel containing 0.66 M formaldehyde (Fluka) and was transferred subsequently to a Zeta-probe membrane (Bio-Rad). Detection of the vWf message was accomplished by

The publication costs of this article were defrayed in part by page charge payment. This article must therefore be hereby marked "*advertisement*" in accordance with 18 U.S.C. §1734 solely to indicate this fact.

Abbreviations: vWd, von Willebrand disease; vWf, von Willebrand factor; FVIII, factor VIII; neo, phosphoglycerate kinase neomycin cassette; ES cells, embryonic stem cells; aPTT, activated partial thromboplastin time.

‖To whom reprint requests should be addressed at: The Center for Blood Research, Harvard Medical School, 800 Huntington Avenue, Boston, MA 02115.

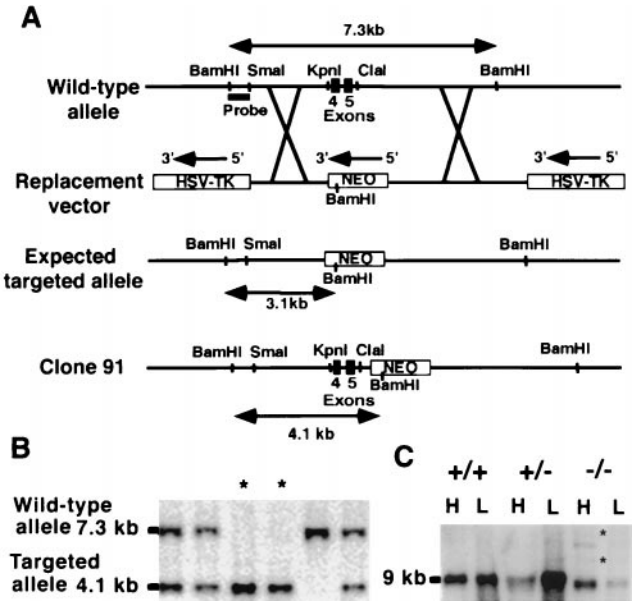

FIG. 1. Targeting of the vWf gene by homologous recombination. (*A*) The wild-type vWf locus is shown on the top. To make the replacement vector, a 800-bp *Kpn*I–*Cla*I fragment including exons 4 and 5 of vWf was deleted and replaced with a 1.7-kb neomycin gene cassette driven by a PGK promoter. The 5′ flanking probe used for screening ES cell clones and genotyping mice by Southern blot analysis is indicated. The probe detects a 7.3-kb *Bam*HI fragment in the wild-type allele and a 3.1-kb *Bam*HI fragment in the expected targeted allele. The bottom line shows the targeted clone actually obtained with the retained *Kpn*I–*Cla*I sites and the neo insertion in intron 5 of vWf. In this clone (clone 91), the probe recognizes a 4.1-kb *Bam*HI fragment. (*B*) Southern blot analysis of genomic DNA isolated from tail biopsies of one litter resulting from heterozygous crossing. DNA was digested with *Bam*HI, electrophoresed, and probed. Fragments recognized from wild-type and targeted alleles are indicated. Two mice are homozygous for the mutation (asterisks). (*C*) Northern blot analysis of vWf RNA: Total RNA was isolated from lung (L) and heart (H) of wild-type, heterozygous, and mutant mice. The vWf probe used was a 1-kb fragment from exon 28 of murine vWf cDNA. Several transcripts are present in the −/− mice. The bands indicated by asterisks also hybridized with a neo probe.

probing with a mouse vWf fragment spanning 1 kb of exon 28 (11), kindly provided by D. Ginsburg (University of Michigan, Ann Arbor, MI). Prehybridization and hybridization were done as for Southern blot analysis.

Immunofluorescence Staining. Mice were killed, and the hearts were frozen immediately in OCT (Miles). Warmed OCT was infused intratracheally, and portions of lung also were frozen in OCT. Sections were fixed in 3.7% formaldehyde (Stephens Scientific, Riverdale, NJ) and were permeabilized in 0.5% Triton X-100 in PBS without divalent cations. The sections were incubated for 30 min at 37°C with rabbit polyclonal antibodies to human mature vWf 1:100 (American Bioproducts, Parsipanny, NJ), to the N- and C-terminal halves of human vWf 1:50 (gift of D. Meyer, Institut National de la Santé et de la Recherche Médicale, Paris), or to human vWf propeptide 1:10 (antibody Mango, gift of R. Montgomery, The Blood Center of Southeastern Wisconsin, Milwaukee, WI), followed by a 30-min incubation with fluorescein-conjugated sheep antibody to rabbit Igs 1:200 (Cappel). Immunofluorescence on blood smears was accomplished in the same way.

ELISA. Blood was obtained by retro-orbital venous plexus sampling in polypropylene tubes containing 0.1 vol of 38 mM citric acid, 75 mM trisodium citrate, and 100 mM dextrose. Plasma was prepared by centrifugation of the blood at 2,500 × *g* for 15 min at room temperature. Microtiter plates were coated overnight at 4°C with rabbit anti-human vWf 3 μg/ml in 50 mM sodium carbonate buffer (pH 9.6). Plates were washed three times with 0.14 M NaCl, 20 mM Tris (pH 7.4), 0.1% Tween 20, 0.3% BSA (Sigma), and plasma, diluted 1:1–1:5,000 in 0.1% Tween 20 Tris buffer saline containing 3% BSA, then was incubated in the wells for 2 hr at 37°C. After three washes, the plates were incubated with a polyclonal anti-human vWf coupled to peroxidase (Dako) diluted 1:3,000 in 0.1% Tween 20 Tris buffer saline 3% BSA for 2 hr at 37°C. After washing, *o*-phenylenediamine dihydrochloride (Sigma), 0.5 mg/ml in 50 mM citric acid, 100 mM Na_2HPO_4 (pH 5) in the presence of 0.015% H_2O_2, was added to the wells, and after 10 min, the reaction was stopped by the addition of 2M H_2SO_4. Absorbance was read at 490 nm in an ELISA reader (Bio-Whittaker).

Multimer Analysis. Plasma samples diluted 1:20 in 10 mM of Tris·HCl and 1 mM EDTA (pH 8) containing 2% SDS were layered on 1% agarose gels (Agarose IEF, Pharmacia) poured on Gelbond (FMC). Gel electrophoresis was run horizontally at a constant amperage of 10 mA. The gel was fixed in 25% isopropyl alcohol and 10% acetic acid for 30 min and rinsed. Multimers were revealed by incubating the dried Gelbond with a polyclonal antibody to human vWf labeled with ^{125}I and visualized by autoradiography.

Hematological Analysis and Bleeding Time Measurement. Blood was obtained as described in the ELISA section. Complete blood counts and hematocrit were determined by using an automatic cell counter (Coulter). The bleeding time was measured after severing a 3-mm segment of tail of 8- to 10-week-old mice (12). The amputated tail was immersed in 0.9% isotonic saline at 37°C, and the time required for the stream of blood to stop was defined as the bleeding time. If no cessation of bleeding occurred after 10 min, the tail was cauterized and 600 s was recorded as the bleeding time.

Coagulation Assays and FVIII Determination. For the activated partial thromboplastin time (aPTT) determination, aPTT reagent (Instrumentation Laboratory, Lexington, MA) was added to citrated test plasma and clotting was initiated by the addition of calcium ions. The time necessary for the clotting to occur was recorded. The prothrombin time was determined by adding citrated test plasma to prothrombin time reagent (Instrumentation Laboratory) and by monitoring the formation of a clot.

FVIII was evaluated by two methods: a chromogenic assay and a clotting assay. The chromogenic assay was carried out by using a COAMATIC FVIII kit (Diapharma, Franklin, OH), according to the manufacturer's protocol. For the clotting assay, different dilutions of mouse plasma ranging from 1:10 to 1:100 were added to human FVIII-deficient plasma (Helena Laboratories) and to aPTT reagent. This mixture was incubated 10 min at 37°C, and 25 mM calcium chloride then was added and a stopwatch was started. FVIII activity was determined by comparing the clotting times of the samples to that of a pool of normal mouse plasma.

***In Vivo* Thrombosis Model.** Mouse platelets were isolated from platelet-rich plasma by means of gel filtration on a Sepharose 2B column (Sigma) and were labeled fluorescently by incubating them with calcein acetoxymethyl ester (0.25 μg/ml) (Molecular Probes) for 15 min at room temperature. Male mice 4- to 5-weeks old were injected with the labeled platelets (4–5 10^9/kg) of matching genotype via the lateral tail vein. The mice were anesthetized immediately with tribromoethanol (Aldrich) (0.15 ml/10 g of body weight), and the mesentery was exteriorized gently through a midline abdominal incision. Arterioles (60- to 100-μm diameter) were visualized with a Zeiss Axiovert 135 inverted microscope equipped with a 100-W HBO fluorescent lamp source (OptiQuip, Highland Mills, NY) and a silicon-intensified tube camera (C 2400; Hamamatsu, Middlesex, NJ) connected to an S-VHS video recorder (AG-6730; Panasonic, Matsushita Electric, Japan). The resting blood vessel was recorded for 4 min, then ferric

chloride (30 μl of a 250-mM solution) (Sigma) was applied on top of the arteriole by superfusion, and video recording was resumed for another 10 min. One blood vessel was recorded per animal. Centerline erythrocyte velocity (Vrbc) was measured by using an optical Doppler velocimeter (Microcirculation Research Institute, Texas A&M College of Medicine, College Station, TX) before filming and 10 min after ferric chloride injury. The shear rate was calculated on the basis of Poiseuille's law for a Newtonian fluid: SR = 8 (Vmean/Dv), where Dv is the diameter of the vessel and Vmean is estimated from the measured Vrbc by using the empirical correlation: Vmean = Vrbc/1.6 (13).

Statistical Analysis. Data are presented as mean ± SEM. Statistical significance was assessed by the Student's *t* test.

RESULTS

Generation of vWf-Deficient Mice. To eliminate the vWf gene product in mice, a targeting vector (Fig. 1*A*) was prepared from the 5′ portion of the murine vWf gene by replacing a 0.8-kb genomic fragment containing exons 4 and 5 of vWf with a 1.7-kb neo cassette. The neo cassette and the herpes simplex virus thymidine kinase cassettes provided positive and negative selection, respectively. Genomic DNA from surviving clones was screened by Southern blot analysis. Three independent transfections were performed, and a total of 1,104 clones was screened. A single targeted clone (clone 91) was identified. Detailed characterization of this clone by Southern hybridization confirmed a genomic rearrangement of the vWf gene but also revealed that the expected deletion of exons 4 and 5 had not occurred, resulting in the insertion of the neo cassette in intron 5 of vWf (Fig. 1*A*).

By differentiating the targeted ES cells into endothelial cells and megakaryocytes, we confirmed the inactivation of the vWf gene in this clone, and we proceeded to its injection into C57BL/6J blastocysts to generate chimeric mice. One 30% chimeric male produced germ-line transmission of the genetic defect; heterozygous animals then were bred to produce homozygous animals (Fig. 1*B*). These were born in the normal Mendelian ratio, indicating that disruption of the vWf gene did not result in embryonic lethality. The homozygous mutant mice appeared grossly normal. Their general health and life span appeared normal.

Verification of the Null Phenotype for vWf. By Northern blot hybridization, by using a murine vWf exon 28 probe, we detected a transcript of ≈9 kb in total heart and lung RNA from wild-type and heterozygous mice (Fig. 1*C*). In the vWf-deficient mice, a few transcripts were present, although none of them was the exact size of the wild-type transcript. No vWf protein was visualized in platelets from a knockout mouse by immunofluorescence staining of blood smears, whereas wild-type platelets were strongly positive (Fig. 2 *A* and *B*). Similarly, heart endothelium (Fig. 2*C*) or lung endothelium (not shown) from a wild-type mouse was positive for vWf, showing granular staining characteristic of Weibel–Palade bodies that was absent in sections from homozygous mutant animals (Fig. 2*D*). By Western blot analysis, we have verified that the polyclonal antibody used for staining recognized the A1 domain of vWf, which is critical for its interaction with platelets (not shown).

An antibody directed against the human vWf propolypeptide (Mango) was also unable to detect any antigen in platelets or in lung sections of the mutant mice, in contrast to the wild type (Fig. 2 *E–H*). This antibody recognizes both domains D1 and D2 of the propolypeptide, as indicated by immunofluorescence staining of cells transfected with either domain (14) (not shown). In addition, we have used polyclonal antibodies raised against two proteolytic fragments of vWf: an N-terminal fragment spanning residues 1–1365 and a C-terminal fragment spanning residues 1366–2050. Neither of these antibodies detected any signal in the mutant platelets, in contrast to wild-type platelets (not shown).

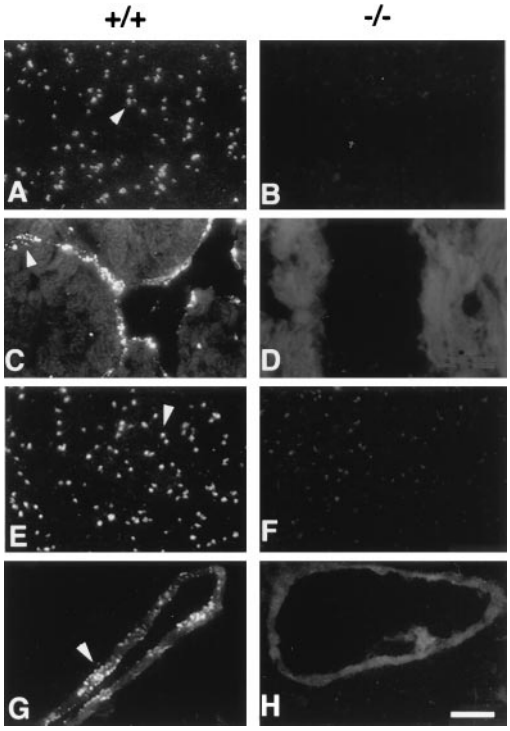

FIG. 2. Immunolocalization of vWf in platelets and tissue sections. Blood smears (*A, B, E,* and *F*), heart sections (*C* and *D*), or lung sections (*G* and *H*) were prepared from wild-type (+/+) and mutant (−/−) mice and stained by immunofluorescence with a polyclonal antibody to mature vWf (*A–D*) or to the propeptide (*E–H*). Bright granular staining characteristic of platelet α-granules (*A* and *E*), and Weibel–Palade bodies (*C* and *G*), stronger than the autofluorescent background of tissue, is observed only in the samples from the wild-type animals (arrowheads). (Bar = 10 μm.)

A highly sensitive ELISA assay that detected the presence of vWf antigen in wild-type plasma up to a 1:5,000 dilution could not detect any signal in homozygous mutant plasma, even at a 1:1 dilution (Table 1). Consistent with the ELISA results, no vWf multimers were detected in the plasma of the mutant mice, whereas a full range of multimers was observed in wild-type and heterozygous mice, comparable to the pattern seen in human plasma (Fig. 3).

Coagulation and Hematological Analysis of vWf-Deficient Mice. After amputation of a portion of the tail, wild-type and

Table 1. Hematological and coagulation analysis of vWf-deficient mice

	+/+	+/−	−/−
vWf antigen, %	96 ± 5.6	49 ± 3.6*	Not detectable
FVIII activity, %	139.5 ± 7.5	81 ± 4*	27.6 ± 1.1*
PT, sec	14.7 ± 0.42	14.8 ± 0.63	14.9 ± 0.67
aPTT, sec	23.2 ± 0.5	24.4 ± 0.4	34.5 ± 1*
Bleeding time, sec	69.7 ± 5.2	91.9 ± 11.2	499 ± 33.4*
Platelets, $\times 10^9$/l	837 ± 43	986 ± 86	931 ± 27
RBC, $\times 10^{12}$/l	7.88 ± 0.12	7.67 ± 0.21	7.72 ± 0.17
WBC, $\times 10^9$/l	2.8 ± 0.33	3.37 ± 0.36	3.07 ± 0.34
Hematocrit, %	37.1 ± 0.6	35.4 ± 1.1	36.9 ± 1
Hemoglobin, g/dl	12.8 ± 0.24	12.4 ± 0.22	12.7 ± 0.31

n = 8–13 mice except for the bleeding time, where n = 15–21. All mice were 2–3 months old. For the ELISA and FVIII activity data, 100% was defined as being the percentage of antigen or activity found in a pool of plasma from 10 C57BL/6J mice. Our mice were on a mixed C57BL/6J/129Sv background, a difference that might account for the higher activity found in our mice compared with the pool.
*$P < 0.0001$ when compared with wild type.

heterozygous mice were able to control their blood loss very quickly and in a similar way, showing that 50% of vWf antigen is sufficient for normal hemostasis (Table 1). In contrast, the vWf-deficient mice presented extensive bleeding. Most animals continued to bleed for as long as they were observed (10 min), and only 5 of 21 mice tested were able to control their blood loss without cauterization. Furthermore, two anesthetized animals that were not cauterized were never able to control their bleeding. No significant differences were found in whole blood samples collected from vWf +/+, vWf −/+, and vWf −/− mice with regard to platelet, red cell and white cell counts, hematocrit, and hemoglobin (Table 1).

In human vWd, the level of coagulation FVIII is closely correlated to the level of vWf. Similarly, in the vWf-deficient mice, the activity level of FVIII is diminished greatly to 20% of wild-type level (Table 1). Interesting to note, similar to humans, the heterozygous animals also have a reduced FVIII activity (57% of wild-type mice). These results were confirmed by a chromogenic assay measuring the level of FVIII in plasma (data not shown). Consistent with the decrease in FVIII, the aPTT test was prolonged in the homozygous mutant animals. As expected, the prothrombin time was not changed (Table 1).

Spontaneous Bleeding Events in vWf-Deficient Mice. We did not observe major bleeding problems in the vWf-deficient mouse colony. The breeding pairs were fertile, and the females survived pregnancy and delivery of normal size litters. There was some evidence, however, that the vWf-deficient mice are susceptible to spontaneous bleeding. A small fraction of vWf −/− neonates (8 of 79 pups monitored, 10.1%) developed visible intra-abdominal bleeding (Fig. 4). When the bleeding did not appear to be massive, the pups recovered and lived normally afterward. For other pups, the bleeding proved fatal. One of the pups examined presented massive hemorrhage in the neck and head area. In addition, 7.2% (4 of 55 mice tested) of the adult knockout mice showed the presence of fecal occult blood, whereas no wild-type mice (45 tested) were positive.

***In Vivo* Thrombosis Model.** The effect of the absence of vWf on thrombus formation was assessed in an *in vivo* model we developed for this purpose. Mice were injected i.v. with fluorescently labeled platelets of the same genotype, and the mesenteric arterioles (60–100 μm in diameter) were examined by intravital microscopy. For these experiments, we chose hemodynamic conditions in which the role of vWf has been demonstrated to be essential (8). The average shear rate of the arterioles we chose to study was 1408 ± 125 s^{-1} (n = 12) for the mutant and 1408 ± 84 s^{-1} (n = 15) for the wild type. Before injury, we did not see any platelet interactions with the arteriole wall in either genotype. A vascular injury was induced by superfusion of 250 mM ferric chloride, which provokes the formation of free radicals leading to the disruption of the endothelium (15). In the wild-type animals, platelet interactions with the injured vessel wall started very quickly. Two minutes after injury, the majority (66.6%) of the wild-type arterioles already presented numerous platelet interactions with the vessel wall (Fig. 5). An example of a wild-type arteriole is presented in Fig. 6*A–D*, where we can follow the progressive increase in the number of platelets interacting with the vessel wall, leading eventually to the complete occlusion of the arteriole. At the end of the 10 min of recording, all of the wild-type arterioles presented either complete occlusion (25%) or numerous platelet interactions with the vessel wall, including formation of thrombi (Fig. 5). In contrast, in the mutant animals, most arterioles (66.6%) had very few, if any, platelet interactions with the vessel wall during the entire period of recording (Fig. 5). Because we detect only labeled platelets, it is possible, although unlikely, that totally unlabeled thrombi would form. However, such thrombi made of several platelets would be seen under light microscopy but, when examined, we did not detect them. The absence of thrombus formation in the mutant animals is not caused by an impaired aggregation of the mutant platelets because they aggregated normally in the presence of ADP (not shown). A typical example of a vWf-deficient arteriole is shown in Fig. 6 *E–H*. Measurement of the shear rate at the end of the 10- min period indicated that there was a trend toward a larger decrease in shear rate in wild-type arterioles (52.7 ± 9.3% of original shear rate) than in vWf-deficient vessels (83.6 ± 13.9% of original shear rate); however, this difference between genotypes was not significant (P = 0.068).

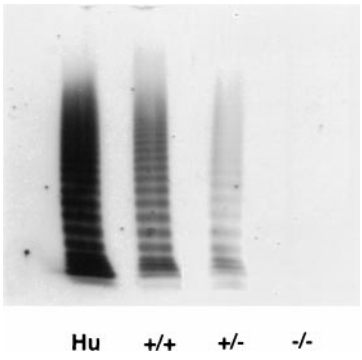

FIG. 3. Analysis of vWf multimers in plasma. Human plasma (Hu) or mouse plasma from wild-type (+/+), heterozygous (±), or homozygous mutant (−/−) mice was layered on an SDS-1% agarose gel. vWf multimers were separated by discontinuous SDS/agarose gel electrophoresis and detected by incubation with ^{125}I-labeled polyclonal anti-human vWf antibody. Autoradiograph of the gel is shown.

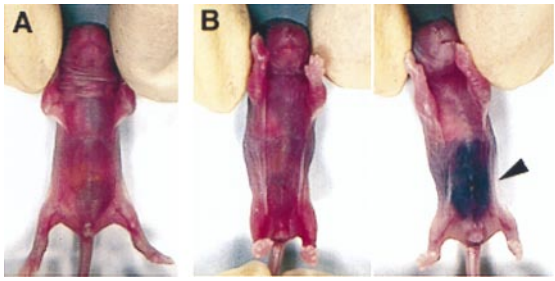

FIG. 4. Spontaneous intra-abdominal bleeding in vWf-deficient 1-day-old pups. (*A*) Wild-type pup. (*B*) Two vWf-deficient littermates. The pup on the right suffered a massive abdominal bleed visible through the skin (arrowhead).

DISCUSSION

The results presented here validate that vWf-deficient mice are a good model of severe human vWd. This mouse strain should prove helpful in future studies of the role of vWf in hemostasis and thrombosis. Dogs and pigs suffering from severe vWd have been described (4) and have clarified some aspects of vWf function. However, some investigations using these models, such as those on atherosclerosis, have yielded more questions than answers and emphasize the need for a small animal model with a defined genetic background.

The gene targeting approach taken to generate vWf-deficient mice led to an unusual recombination/insertion event. Similar failure to obtain the expected deletion has been described in other knockout experiments, such as that leading to the absence of inducible nitric oxide synthase (16). The insertion of neo into an intron rather than an exon sequence also has been reported to lead to a null phenotype in the case of the fibronectin gene (17). It appears that the genomic sequences flanking the exon contain crucial information for correct processing of the message or that the neo sequences themselves interfere with mRNA splicing because no message present in the vWf-deficient mice was of the correct size. Of

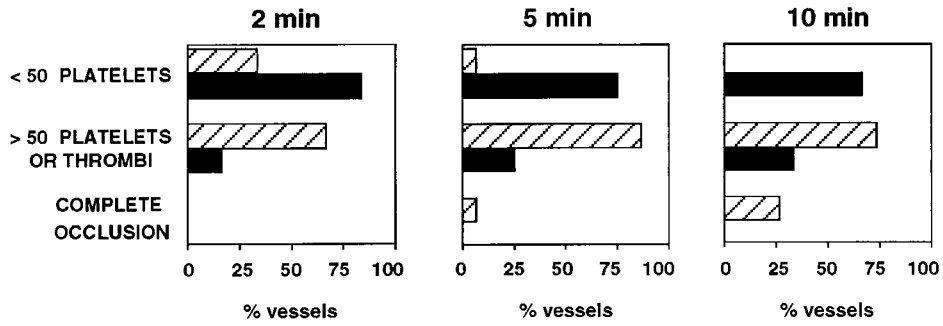

FIG. 5. Platelet-vessel wall interactions after ferric chloride-induced injury. Wild-type (striated columns, $n = 15$) or vWf-deficient mice (black columns, $n = 12$) were injected with fluorescently labeled platelets of matching genotype, and their mesenteries were exposed. Arterioles (60–100 μm in diameter) were selected, and a vascular injury was provoked by superfusion with ferric chloride. Any platelet interaction with the vessel wall, either brief or stable, was counted. The presence of platelet thrombi also was recorded. For each vessel studied, the total number of interactive platelets during the first 2 min, 5 min, or during the entire 10 min of filming was recorded and was classified into categories, as indicated on the left.

importance, these messages apparently were not functional because they did not produce detectable amounts of either vWf or its propolypeptide. Polyclonal antibodies to vWf detected vWf in wild-type plasma even at a 1:5,000 dilution, whereas none of the dilutions of mutant plasma produced a positive signal (Table 1). The antibody used recognizes the functionally important A1 domain encoded by exon 28. Similarly, a polyclonal antibody to the propolypeptide (von Willebrand antigen II), which recognizes both domains of the propolypeptide, D1 and D2, also did not react with mutant tissues, whereas wild-type specimens gave a strong positive signal (Fig. 2). Therefore, no proteins containing either the propolypeptide or the mature vWf antigen were detectable in the mutant mice.

The vWf-deficient mice are born in the correct Mendelian ratio, demonstrating that vWf is not essential for normal embryonic development. Approximately 10% of the vWf-deficient neonates develop intra-abdominal bleeding, which can be fatal. After the neonatal period, no obvious spontaneous bleeding seems to be associated with the vWf-deficiency, and the mutant mice survive even challenging episodes, such as pregnancy and delivery. This finding is consistent with other gene targeting studies in which the absence of FVIII or factor IX leads to a milder phenotype in mice as compared with humans (18–20). However, it should be taken into account that laboratory mice have a relatively protected existence and may be less prone to injury than human patients. In any of these mouse models, a deliberate injury can lead to uncontrolled bleeding and death from hemorrhage.

Mice lacking fibrinogen show a similar but somewhat more severe tendency to bleed than do the vWf-deficient mice (21). Fibrinogen and vWf are both ligands for the platelet receptor αIIbβ3, and both are involved in platelet aggregation and thrombus formation. Fibrinogen can support platelet adhesion and aggregation at low shear rates, whereas at high shear rates, vWf is essential for both platelet adhesion and aggregation (ref. 8; Fig. 5 and 6). Despite the similar roles played by fibrinogen and vWf, the phenotype of the fibrinogen-deficient mice is more severe, probably because of the involvement of fibrinogen in fibrin clot formation. A more relevant comparison can be made between the vWf-deficient mice and mice that lack the fibrinogen motif responsible for binding to αIIbβ3 but retain the clotting function (22). These mice display a milder phenotype resembling our vWf-deficient mice. Despite the moderate phenotype observed in the vWf-deficient mice, it is clear that vWf is critical to controlling bleeding because even a minor surgical procedure such as snipping 3 mm of the tip of the tail can lead to fatal hemorrhage.

An important feature of human type 1 vWd (decreased vWf level) is reduced FVIII, the concentration of which usually parallels that of vWf even though there is a considerable molar excess of binding sites provided by the remaining vWf (23–25). The close relationship between the plasma concentrations of the two proteins is still a mystery. The vWf-deficient mice will be a good model to study the regulation of FVIII by vWf. Their FVIII level is relatively low (20% of wild type), and there is very little variation between animals (Table 1). In addition, the

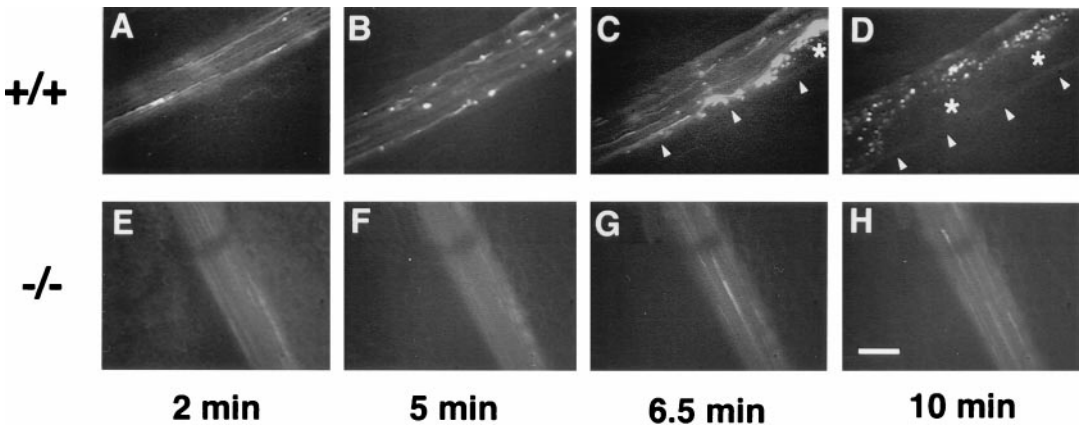

FIG. 6. *In vivo* thrombosis model in arterioles after ferric chloride-induced injury. An arteriole from a wild-type (+/+) or a vWf-deficient (−/−) mouse was injured by ferric chloride superfusion and photographed at four time points after injury. A progression in the quantity of platelets interacting with the vessel wall is visible in the wild-type arteriole (*A–D*), leading to complete occlusion and blood stasis in *D*. Arrowheads in *C–D* show edge of vessel above which is the forming thrombus. Asterisks indicate the center of a thrombus containing unlabeled and bleached platelets. Almost no platelet interactions are visible in the vWf-deficient arteriole (*E–H*). (Bar = 50 μm.)

heterozygous mice that have half normal amounts of vWf antigen also have decreased FVIII activity, down to 57% of the wild type, mimicking human patients with type 1 vWd.

To study the role of vWf in thrombosis, we developed an *in vivo* thrombosis model by using intravital microscopy, which allowed us to follow "live" the platelet interactions with the injured vessel wall, as well as the formation of thrombi. We conducted these experiments in arterioles at high shear rates, conditions in which the vWf-glycoprotein Ib axis is essential for the initial platelet adhesion (8). In the majority of vWf-deficient mice, we did not see any platelets interacting with the injured vessel. This finding confirmed the requirement for vWf in the first steps of platelet thrombus formation at high shear rates. However, thrombus formation occurred in a minority of vWf-deficient vessels. This happened through a vWf-independent mechanism, possibly caused by temporary or stable changes in the hemodynamic conditions present in the injured arterioles, leading to the intervention of other platelet receptors such as αIIbβ3 or the β1 integrins. This vascular injury model will allow us to evaluate the role of other adhesion molecules in thrombus formation in both arterioles and venules and to compare their relative importance. Such an intravital model also will allow testing of the efficacy of thrombotic inhibitors, leading to the potential development of better anti-thrombotic agents.

The vWf-deficient mice described in this study represent a very close model of severe vWd in humans, with the accompanying hemostatic and thrombotic defects. These mice will be useful to test the potency of various vWf/FVIII preparations in hemostasis and eventually gene therapy methods. Finally, the availability of these mice will allow testing of the involvement of vWf in important diseases, such as atherosclerosis (6) and cancer metastasis (26), and other pathological conditions involving platelet adhesion or thrombus formation.

We thank Drs. Livingston Van De Water and Corine Reimer for the ES cell differentiation protocol; Dr. Robert Montgomery for the antibodies to the propolypeptide; Dr. Zaverio Ruggeri for providing the A1 domain polypeptide; Dr. David Ginsburg for the exon 28 probe; Pr. Dominique Meyer for the antibodies to the proteolytic fragments of vWf; Susan Chapman for heart and lung sections, and Lesley Cowan for assistance with preparation of the manuscript. This work was supported in part by National Institutes of Health Grants R01 HL41002 (to D.D.W.) and HL41484 (to R.O.H.). R.O.H. is an Investigator of the Howard Hughes Medical Institute. P.S.F. is supported by a fellowship from the Medical Research Council of Canada.

1. Ewenstein, B. M. (1997) *Annu. Rev. Med.* **48,** 525–542.
2. Andrews, R. K., Lopez, J. A. & Berndt, M. C. (1997) *Int. J. Biochem. Cell Biol.* **29,** 91–105.
3. Weiss, H. J., Sussman, I. I. & Hoyer, L. W. (1977) *J. Clin. Invest.* **60,** 390–404.
4. Bowie, E. J. & Owen, C. A. (1989) in *Coagulation and Bleeding Disorders*, eds. Zimmerman, T. S. & Ruggeri, Z. M. (Dekker, New York), pp. 305–324.
5. Wu, Q. Y., Drouet, L., Carrier, J. L., Rothchild, C., Berard, M., Rouault, C., Caen, J.-P. & Meyer, D. (1987) *Arteriosclerosis* **7,** 47–54.
6. Nichols, T. C., Bellinger, D. A., Davis, K. E., Koch, G. G., Reddick, R. L., Read, M. S., Rapacz, J., Hasler-Rapacz, J., Brinkhous, K. & Griggs, T. R. (1992) *Am. J. Pathol.* **140,** 403–415.
7. Sakariassen, P. G., Arts, P. A. M. M., de Groot, P. G., Houjdlik, W. P. M. & Sixma, J. J. (1983) *J. Lab. Clin. Med.* **102,** 522–535.
8. Ruggeri, Z. M. (1997) *Thromb. Haemostasis* **78,** 611–616.
9. Mayadas, T. N., Johnson, R. C., Rayburn, H., Hynes, R. O. & Wagner, D. D. (1993) *Cell* **74,** 541–554.
10. Bradley, A. (1987) in *Teratocarcinoma and Embryonic Stem Cells: A Practical Approach*, ed. Robertson, E. J. (IRL, Oxford), pp. 113–151.
11. Nichols, W. C., Cooney, K. A., Mohlke, K. L., Ballew, J. D., Yang, A., Bruck, M. E., Reddington, M., Novak, E. K., Swank, R. T. & Ginsburg, D. (1994) *Blood* **83,** 3225–3231.
12. Subramaniam, M., Frenette, P. S., Saffaripour, S., Johnson, R. C, Hynes, R. O. & Wagner, D. D. (1996) *Blood* **87,** 1238–1242.
13. Baker, M. & Wayland, H. (1974) *Microvasc. Res.* **7,** 131–143.
14. Journet, A. M., Saffaripour, S. & Wagner, D. D. (1993) *Thromb. Haemostasis* **70,** 1053–1057.
15. Zuccarello, M. & Anderson, D. K. (1989) *Stroke (Dallas)* **20,** 367–371.
16. Wei, X-Q., Charles, I. G., Smith, A., Ure, J., Feng, G.-J., Huang, F.-P., Xu, D., Muller, W., Moncada, S. & Liew, F. Y. (1995) *Nature (London)* **375,** 408–411.
17. Georges-Labouesse, E. N., George, E. L., Rayburn, H. & Hynes, R. O. (1996) *Dev. Dyn.* **207,** 145–156.
18. Bi, L., Lawler, A. M., Antonarakis, S.E., High, K. A., Gearhart, J. D. & Kazazian, H. H., Jr. (1995) *Nat. Genet.* **10,** 119–121.
19. Bi, L., Sarkar, R., Naas, T., Lawler, A. M., Pain, J., Shumaker, S. L., Bedian V. & Kazazian, H. H., Jr. (1996) *Blood* **88,** 3446–3450.
20. Wang, L., Zoppè, M., Hackeng, T. M., Griffin, J. H., Lee, K.-F. & Verma, I. M. (1997) *Proc. Natl. Acad. Sci. USA* **94,** 11563–11566.
21. Suh, T. T., Holmbäck, K., Jensen, N. J., Daugherty, C. C., Small, K., Simon, D. I., Potter, S. S. & Degen, J. L. (1995) *Genes Dev.* **9,** 2020–2033.
22. Holmbäck, K., Danton, M. J. S., Suh, T. T., Daugherty C. C. & Degen, J. L. (1996) *EMBO J.* **15,** 5760–5771.
23. Lollar, P., Hills-Eubanks, D. C. & Parker, C. G. (1988) *J. Biol. Chem.* **263,** 10451–10455.
24. Hoyer, L. W. (1981) *Blood* **58,** 1–13.
25. Holmberg, L. & Nilsson, I. M. (1992) *Eur. J. Haematol.* **48,** 127–141.
26. Nierodzik, M. L., Klepfish, A. & Karpatkin, S. (1995) *Thromb. Haemostasis* **74,** 282–290.